Journal of Applied Sciences

ISSN 1812-5654

science alert

ANSInet
an open access publisher
http://ansinet.com

Journal of Applied Sciences 14 (22): 2892-2908, 2014
ISSN 1812-5654 / DOI: 10.3923/jas.2014.2892.2908

A Fuzzy Controller for Driving the Electric Personal Vehicle PICAV

[1]R.M. Molfino, [1]M. Zoppi and [2]E.M. Cepolina
[1]Industrial Robot Design Research Group, University of Genova,
Via all'Opera Pia, 15A, 16145 Genova, Italy
[2]Department of Civil Engineering, Vie e Trasporti, University of Pisa, Italy

Abstract: In this study, the authors developed a full electric personal vehicle and studied its mobility behaviour under autonomous or semi-autonomous driving. For this goal a fuzzy controller, encoding the reactive behaviour of the vehicle, has been studied to steer the vehicle by generating the commands for the four in-wheel actuators so that the vehicle follows the planned trajectory as closely as possible, with good stability margins. Due to the novelty of the vehicle architecture, the vehicle kinematic and dynamic models, have been purposely developed in order to reconstruct the vehicle real mobility in different scenarios. These models have been used to setup the new fuzzy control system in simulation before its implementation on the vehicle. The study presents the vehicle mobility and control models and the results achieved in simulation as well as the early experimental results obtained with the second prototype of the Personal Intelligent City Accessible Vehicle (PICAV) developed within the PICAV European Project.

Key words: Electric vehicle, single-user vehicle, assisted driving, 4WD vehicle modelling, mobile platform, fuzzy logic, control architectures

INTRODUCTION

In the last ten years there has been great efforts to create green zones in downtown areas, in tourist areas and public parks, ensuring citizens have an economic, social and environmentally sustainable mobility system. A particular attention has to be dedicated to guarantee the right to mobility for all people, avoiding any kind of social exclusion and changes in personal habits, culture and quality of life, especially for less able (elderly or handicapped) users who cannot resort to the typical efficient and clean walking and cycling mobility resources powered by human muscles. So the need to develop sustainable, easy to drive, personal mobility vehicles.

The problem of personal urban mobility has been considered in this decade and several valuable developments have, already, been undertaken, as reported in (Mitchell *et al*., 2010). In the following some significant personal vehicles are briefly introduced.

The Personal Mobility PM-01 of Toyota targets the driver-vehicle unity, with ergonomic focus, separated cabin and wheel-suspension structure allowing the PM to vary its posture according to the speed and to facilitate the entry and exit.

A development of the PM-01, the i-UNIT, is characterised by its exoskeleton design; it offers personal mobility in an ultra-compact size with variable positioning as the PM (Kato *et al*., 2006); drive-by-wire technology and handling enable the passenger to make on-the-spot turns (curves with zero radius, the vehicle turns in a circle, keeping its center in the same spot on the ground) and drive at high speed at will.

The i-REAL is a personal mobility vehicle made closely in human scale that Toyota proposes for commercialization in the near future; it uses three wheels in low-speed mode, shortening its wheelbase to allow manoeuvring naturally among pedestrians; in high-speed mode the wheelbase lengthens to provide a lower centre of gravity and better driving performance.

The Human Transporter SEGWAY HT can self-balance with a technology called dynamic stabilisation using a set of solid-state gyroscopes, tilt sensors, high-speed microprocessors and electric motors performing to keep it balanced whether travelling at 4.5 m sec^{-1}, carrying a heavy load, slowly manoeuvring in tight spaces, or standing still (Sawatzky *et al*., 2007).

NOAH is a high performance Segway influenced concept personal vehicle that reacts to driver's movements, determining the acceleration, braking and turning.

The Smart Cities group at the MIT Media Laboratory developed the MIT CITY CAR, in collaboration with Frank Gehry and General Motors (Lark, 2005), based upon principles very similar to the ones of the PICAV: it is a

Corresponding Author: R.M. Molfino, Industrial Robot Design Research Group, University of Genova,
Via all'Opera Pia, 15A, 16145 Genova, Italy

lightweight electric vehicle that embeds in each of its four wheels an electric motor; steering and braking mechanisms, suspension and digital controls, are all integrated into modules that can be snapped on and off.

A three wheels car concept was designed by David Varga for Peugeot: it is a two-seater electric vehicle with a third wheel improving stability. The car is perfect for crowded parking lots and is easy to manoeuvre.

The Smera of Lumeneo is a two seat, four wheel electric vehicle that is narrow enough (0.8×2.4 m) to manoeuvre as a motorcycle (Grzegozek, 2010).

Personal Intelligent City Accessible Vehicle (PICAV) differs from these vehicles because it is designed to move, also in uneven steep grounds, weak (old and disabled) people for which the need of motion stability and manoeuvring softness in any terrain conditions is of primary importance.

The PICAV is a personal vehicle designed to ensure accessibility for all in urban pedestrian environments. It can be used by normally able people as well as the elderly or handicapped. Ergonomics, comfort, the small dimensions, tiny footprint, stability, assisted driving, eco-sustainability, parking and mobility dexterity as well as vehicle/infrastructures intelligent networking are the main drivers of the PICAV design.

The application fields of PICAV are outdoor pedestrian environments where usual public transport services cannot operate because of the width and slope of the infrastructures, uneven pavements including steps and the interactions with high pedestrian flows. It is equipped with sensors to monitor the drive and ensure the safety of passengers and pedestrians (Cepolina and Farina, 2012a; Cepolina and Tyler, 2001).

The main characteristics of PICAV are: small footprint 800x1200 mm, 400 kg weight (batteries included), four independently wheels drive (4WD), 25 km h^{-1} max speed. The real and virtual prototypes of PICAV are illustrated in Fig. 1.

The PICAV control needs to grant stable and friendly driving conditions, within the wide range of grounds the vehicle has to travel. The aim is to design control systems efficient and robust for uncertain non linear multi body mechanisms. The uncertainty depends on the complexity of the reference architecture (the car is composed of a relevant number of bodies, with multiple compliant joints), on the nonlinearity of the process dynamics (the coupled inertial effects have stability outcomes), on the variability of the forcing terms (the influences of payloads, ground-tyres interactions, external disturbances, etc.,) and on the redundancy of the actuation system (the four wheels and the two steering independent motors).

Car manufacturers are certainly well aware of the recalled uncertainty and operate with empirical data gathered from previous experiences, slightly modifying already developed cars, to improve the actual performance of the newly offered models.

On the robotic side, many 4WD mobile platforms have been developed but our problem is different because: The presence of the human passenger on board requires smooth and stable behaviour all along different travel and ground conditions; the driver behaves in different ways in different traffic conditions; the range of manoeuvres in personal vehicles is wider than in mobile platforms where autonomous driving can choose to use small angles ranges justifying the linearity of the control. For this reason a detailed realistic dynamic model has been developed in order to assess the proposed fuzzy controller parameters in different conditions and environments, making the control more accurate, robust and efficient.

The study presents in detail the model used to describe the dynamics of the PICAV, driven, along planned rectilinear and curved paths, on different environments with even and uneven ground. The car body may present unbalances due to asymmetric mass distribution, resulting in non-diagonal mass moments of

Fig. 1(a-b): PICAV-2 (a) Physical prototype and (b) Digital mock-up

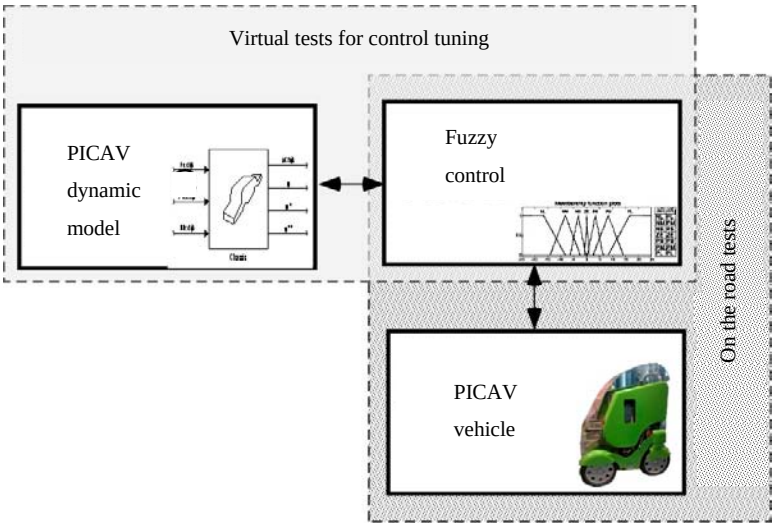

Fig. 2: Schema for the fuzzy control design process

inertia; the independent driving wheels are connected by means of non linear suspensions.

The supervising controller regulates the speed and the torque of each wheel, to assure balanced steering conditions to the driver. It is structured with a hierarchical architecture. The lower layer performs the adaptive control of the wheels actuation with closure of the feedback through, at the intermediate layer, a fuzzy logic decision scheme. The higher layer is ruled by a driver or, for automatic navigation applications, by a trajectory planning block (Fig. 2).

The design and implementation of a high performance control strategy is a difficult problem that can be best solved by exploiting a deep knowledge of the vehicle kinematic and dynamic behaviour. For this reason vehicle model is dedicated to the reconstruction of a PICAV vehicle accurate model that served as the basis for the control system development.

Very often the robotic community proposed and developed mobile platforms optimal control systems in the state variables solving typical least square problems to optimize multi-objectives performance indexes. In general these methods resort to vehicle linear or bilinear models, like quarter car model, half car model, single-track model with a limited number of degrees of freedom and heavy approximations that make them to reconstruct the vehicle real behaviour in limited ranges of the state variables values. Common characteristics of these models is that they describe only part of the vehicle dynamics limiting to particular features of the vehicle motion. So the control systems in general are defined separately for the longitudinal, transversal, yaw or suspensions motions.

VEHICLE MODEL

The PICAV vehicle presents a closed-loop dynamics, with steering, acceleration and braking commands selected by the driver. Traction (or braking) forces are related to interactions between tyres and road; actual friction, combined to distributed vertical loads, is usually sufficient to transfer motors' torque into driving components. Unbalanced reactions result in tyre creeping and rubbing with unwanted car drift and extra steering for not deviating from the selected course.

A nonlinear vehicle model with 18 DOF's, with possibility of autonomous four-wheel driving and two-wheel steering was used as reference virtual vehicle for the control assessment, parameters estimation and simulation (Michelini *et al*., 2001a). The mentioned model describes motion of the vehicle mass centre (G) in three coordinate directions and three rotations of the vehicle about its main axes of inertia. Also, the model describes dynamics of the Vehicle Suspension System (VSS) on all four wheels in the vertical direction, as well as the tire dynamics. Each wheel possesses, beside vertical deflection, two extra DOF's: Rotation about the horizontal axis with angular velocity Ω_i, i = 1, ...4 and rotation about the vertical axis with respect to the road surface. The second rotation represents a change of the ground steering angle δ_i, i = 1, 2. The vehicle body model is determined by rigid body dynamics, while the model of the suspension system is described by the behaviour of a mass spring damper system. Tire model is determined by a nonlinear, functional dependence between the longitudinal and lateral tire-road interaction forces, respectively and a tire side slip ratio, i.e., the corresponding tire side slip angle. The used vehicle

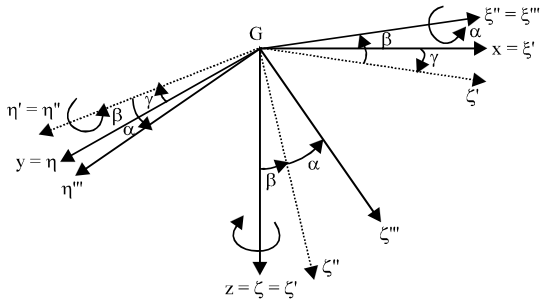

Fig. 3: Mobile frames: yaw γ, pitch β, roll α aerodynamic angles

model is based on the modified model of (Rodic and Vukobratovic, 1996), that has been structurally rearranged and extended by relaxing approximations on small roll and pitch angles as well as considering road elevation.

The defined model is valid in the case when the following assumptions can be adopted: (1) The vehicle body represents a rigid body in a mechanical sense, supported by the road surface with four elastic subsystems, representing the VSS; (2) Each VSS possesses elastic properties only in the vertical direction (perpendicular to the road surface), while it is considered that it is absolutely rigid in the longitudinal and lateral directions.

Vehicle reference frames: The PICAV vehicle is made up by a body, carried by 4 motor-wheels (Fig. 1).

The first approximation kinematic model deals with a solid body, whose centre of mass G moves along a planar path and varying local drift angle. The following reference axes, shown in Fig. 3, are considered:

O {XYZ} = fixed frame
G {xyz} = Mobile frame, preserving the attitude of O {XYZ}
G {ξη ξ} = Varying attitude body-frame, principal of inertia

The angular velocity components are expressed either in the body-axes or in the fixed or only-translating-axes, by:

$$\begin{bmatrix}\omega_\xi\\ \omega_\eta\\ \omega_\zeta\end{bmatrix}=\begin{bmatrix}\cos\beta\cos\gamma & \cos\beta\sin\gamma & -\sin\beta\\ \sin\alpha\sin\beta\cos\gamma-\cos\alpha\sin\gamma & \sin\alpha\sin\beta\sin\gamma+\cos\alpha\cos\gamma & \sin\alpha\cos\beta\\ \cos\alpha\sin\beta\cos\gamma+\sin\alpha\sin\gamma & \cos\alpha\sin\beta\sin\gamma-\sin\alpha\cos\gamma & \cos\alpha\cos\beta\end{bmatrix}\begin{bmatrix}\omega_x\\ \omega_y\\ \omega_z\end{bmatrix} \quad (1)$$

$$\begin{bmatrix}\omega_x\\ \omega_y\\ \omega_z\end{bmatrix}=\begin{bmatrix}\cos\beta\cos\gamma & \sin\alpha\sin\beta\cos\gamma-\cos\alpha\sin\gamma & \cos\alpha\sin\beta\cos\gamma+\sin\alpha\sin\gamma\\ \cos\beta\sin\gamma & \sin\alpha\sin\beta\sin\gamma+\cos\alpha\cos\gamma & \cos\alpha\sin\beta\sin\gamma-\sin\alpha\cos\gamma\\ -\sin\beta & \sin\alpha\cos\beta & \cos\alpha\cos\beta\end{bmatrix}\begin{bmatrix}\omega_\xi\\ \omega_\eta\\ \omega_\zeta\end{bmatrix} \quad (2)$$

Such components are related to the time variations of the yaw, pitch and roll angles, by:

$$\begin{bmatrix}\omega_\xi\\ \omega_\eta\\ \omega_\zeta\end{bmatrix}=\begin{bmatrix}\dot\alpha\\ 0\\ 0\end{bmatrix}+\begin{bmatrix}1 & 0 & 0\\ 0 & \cos\alpha & \sin\alpha\\ 0 & -\sin\alpha & \cos\alpha\end{bmatrix}\begin{bmatrix}0\\ \dot\beta\\ 0\end{bmatrix}+\begin{bmatrix}\cos\beta & 0 & -\sin\beta\\ \sin\alpha\sin\beta & \cos\alpha & \sin\alpha\cos\beta\\ \cos\alpha\sin\beta & -\sin\alpha & \cos\alpha\cos\beta\end{bmatrix}\begin{bmatrix}0\\ 0\\ \dot\gamma\end{bmatrix} \quad (3)$$

$$\begin{bmatrix}\omega_x\\ \omega_y\\ \omega_z\end{bmatrix}=\begin{bmatrix}\dot\alpha\\ 0\\ 0\end{bmatrix}+\begin{bmatrix}1 & 0 & 0\\ 0 & \cos\alpha & -\sin\alpha\\ 0 & \sin\alpha & \cos\alpha\end{bmatrix}\begin{bmatrix}0\\ \dot\beta\\ 0\end{bmatrix}+\begin{bmatrix}\cos\beta & \sin\alpha\sin\beta & \cos\alpha\sin\beta\\ 0 & \cos\alpha & -\sin\alpha\\ -\sin\beta & \sin\alpha\cos\beta & \cos\alpha\cos\beta\end{bmatrix}\begin{bmatrix}0\\ 0\\ \dot\gamma\end{bmatrix} \quad (4)$$

With almost-rigid suspensions (small oscillations), the approximations hold:

$$\omega_\xi \approx \dot\alpha-\beta\dot\gamma \qquad \omega_\eta \approx \dot\beta+\alpha\dot\gamma \qquad \omega_\zeta \approx \dot\gamma-\alpha\dot\beta \quad (5)$$

$$\omega_x \approx \dot\alpha+\beta\dot\gamma \qquad \omega_y \approx \dot\beta-\alpha\dot\gamma \qquad \omega_z \approx \dot\gamma+\alpha\dot\beta \quad (6)$$

The corresponding yaw, pitch and roll angular rates become:

$$\dot\alpha \approx \omega_\xi+\frac{\beta}{1+\alpha^2}(\omega_\zeta+\alpha\omega_\eta) \qquad \dot\beta \approx \frac{1}{1+\alpha^2}(\omega_\eta-\alpha\omega_\zeta) \qquad \dot\gamma \approx \frac{1}{1+\alpha^2}(\omega_\zeta+\alpha\omega_\eta) \quad (7)$$

$$\dot\alpha \approx \omega_x-\frac{\beta}{1+\alpha^2}(\omega_z-\alpha\omega_y) \qquad \dot\beta \approx \frac{1}{1+\alpha^2}(\omega_y+\alpha\omega_z) \qquad \dot\gamma \approx \frac{1}{1+\alpha^2}(\omega_z-\alpha\omega_y) \quad (8)$$

or, suppressing the second order couplings:

$$\dot\alpha \approx \omega_\xi+\beta\omega_\zeta \qquad \dot\beta \approx \omega_\eta-\alpha\omega_\zeta \qquad \dot\gamma \approx \omega_\zeta+\alpha\omega_\eta \quad (9)$$

$$\dot\alpha \approx \omega_x-\beta\omega_z \qquad \dot\beta \approx \omega_y+\alpha\omega_z \qquad \dot\gamma \approx \omega_z-\alpha\omega_y \quad (10)$$

These expressions are exploited to locally integrate the angular displacements in yaw, pitch and roll, when the angular speed components are known.

VEHICLE KINEMATIC MODEL

Backward kinematics: PICAV is a low speed vehicle and the Ackerman kinematic steering conditions are satisfied (Saiz-Rubio *et al*., 2013).

With reference to Fig. 4 the following relations hold:

$$\frac{V_G}{R_G}=\frac{V_1}{R_1}=\frac{V_2}{R_2}=\frac{V_3}{R_3}=\frac{V_4}{R_4} \quad (11)$$

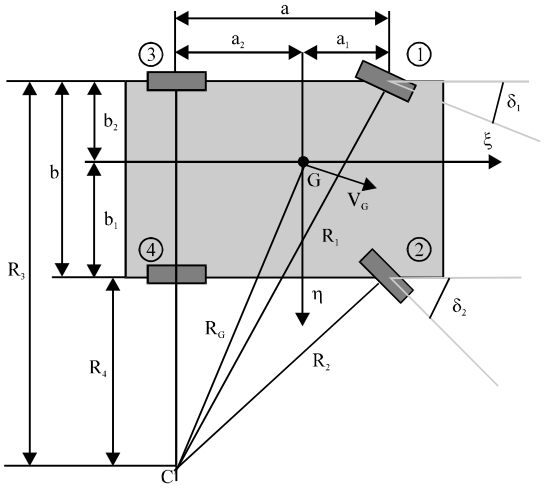

Fig. 4: Main vehicle dimensions and kinematic steering schema

where, in V_i, i = 1-4, are the velocities of the ith wheel center and R_i are the bending radiuses of the wheels trajectories; V_G is the centroid's velocity and R_G is the bending radius of the centroid's path:

$$R_G = \sqrt{(\text{acotg}\,\delta_1 - b_2)^2 + (a_2)^2} \tag{12}$$

Since the chassis is symmetric ($a_1 \cong a_2 \cong 0.5a$) and $\text{cotg}_\delta = \text{cotg}\delta_2 - b/a$ (with δ_1 and δ_2 the steering angles), then R_G is expressed by:

$$R_G = \sqrt{(\text{acotg}\,\delta_1 - 0.5b)^2 + (0.5a)^2}$$

By calling R_0 the rolling radius of the tyres, the reference angular velocity of each wheel is found to be:

$$\Omega_i^{id} = \frac{V_G}{R_G R_0} R_i \tag{13}$$

In the case of two steering front wheels, as indicated in Fig. 4, the individual bending radiuses, written as functions of the trajectory variables δ_1, V_G and the vehicle parameters, are:

$$\begin{aligned} R_1 &= a/\text{sen}\delta_1 \\ R_2 &= a\sqrt{(\text{cotg}\,\delta_1 - b/a)^2 + 1} \\ R_3 &= a\,\text{cotg}\,\delta_1 \\ R_4 &= a\,\text{cotg}\,\delta_1 - b \end{aligned} \tag{14}$$

And the corresponding motor wheels reference velocities are:

$$\begin{aligned} \Omega_1^{id} &= \frac{V_G}{R_0}\frac{a}{\text{sen}\delta_1}\frac{1}{\sqrt{(\text{acotg}\delta_1 - b_2\,\text{sign}(\delta_1))^2 + a_2^2}} \\ \Omega_2^{id} &= \frac{V_G}{R_0}\frac{1}{\sqrt{(\text{acotg}\delta_1 - b_2\,\text{sign}(\delta_1))^2 + a_2^2}}\sqrt{\left(\frac{a}{\text{tg}\delta_1} - \text{sign}(\delta_1)b\right)^2 + (a)^2} \\ \Omega_3^{id} &= \frac{V_G}{R_0}\frac{a}{\text{tg}\delta_1}\frac{1}{\sqrt{(\text{acotg}\delta_1 - b_2\,\text{sign}(\delta_1))^2 + a_2^2}} \\ \Omega_4^{id} &= \frac{V_G}{R_0}\frac{1}{\sqrt{(\text{acotg}\delta_1 - b_2\,\text{sign}(\delta_1))^2 + a_2^2}}\left(\frac{a}{\text{tg}\delta_1} - \text{sign}(\delta_1)b\right) \end{aligned} \tag{15}$$

In vehicle control problem the input variables describing the wanted trajectory are the time laws of δ_1 and V_G.

Platform kinematics: Referring to the vehicle platform, the suspensions are located at P_1, P_2, P_3, P_4. The velocities of the points P_i bear the form:

$$V_{P_i} = \begin{bmatrix} u \\ v \\ w \end{bmatrix} + \begin{bmatrix} 0 & -\omega_\zeta & \omega_\eta \\ \omega_\zeta & 0 & -\omega_\xi \\ -\omega_\eta & \omega_\xi & 0 \end{bmatrix} \begin{bmatrix} \xi_i \\ \eta_i \\ \zeta_i \end{bmatrix} \tag{16}$$

Where:

$$v_G = (u\ v\ w)^T;\ [\omega_\xi\ \omega_\eta\ \omega_\zeta]^T$$

is given in Eq. 3:

$$(P_i\text{-}G) = (\xi_i\ \eta_i\ \zeta_i)^T$$

It represents the position of the four actuation points:

$$\begin{aligned} (P_1 - G) &= [\xi_1\ \ \eta_1\ \ \zeta_1]^T = [\,a_1\ \ -b_2\ \ c]^T \\ (P_2 - G) &= [\xi_2\ \ \eta_2\ \ \zeta_2]^T = [\,a_1\ \ b_1\ \ c]^T \\ (P_3 - G) &= [\xi_3\ \ \eta_3\ \ \zeta_3]^T = [-a_2\ \ -b_1\ \ c]^T \\ (P_4 - G) &= [\xi_4\ \ \eta_4\ \ \zeta_4]^T = [-a_2\ \ b_2\ \ c]^T \end{aligned} \tag{17}$$

The related drift angles are approximately given by:

$$\varphi_i = \text{artn}\frac{v + \dot\gamma\,\xi_i + \beta\,\dot\gamma\,\zeta_i}{u - \dot\gamma\,\eta_i + \alpha\,\dot\gamma\,\zeta_i} \approx \frac{v + \dot\gamma\,\xi_i}{u - \dot\gamma\,\eta_i} \tag{18}$$

Result that shows the negligible dependence from the transversal interaxis distance b, when the component u of the G speed is (comparatively) large.

VEHICLE DYNAMIC MODEL

The nonlinear dynamic model of a vehicle, like the second PICAV version, with two axes, four independent

motor wheels and two steering front wheels is derived considering the vehicle as a system with nine degrees of freedom: The longitudinal motion along the platform ξ axis, the transversal motion along the platform η axis, the roll, pitch and yaw motions around the ξ, η, ζ axes and the wheels four motions. The model is complex, non-linear and exhibits dynamic couplings between the motions.

The aerodynamics lifting effects are neglected because of the PICAV slow speed, the vehicle weight is assumed to be shared out by front and rear axles, ξ, η, ζ axes are principal of inertia of the vehicle:

$$I_{ch} = \text{diag}(I_{ch\xi}\ I_{ch\eta}\ I_{ch\zeta})$$

With the approximation hypotheses the motion equations can be written as:

$$\begin{aligned}
&\sum_{i=1}^{4} F_{\xi i} - F_{\xi g} = m_T a_\xi \\
&\sum_{i=1}^{4} F_{\eta i} = m_T a_\eta \\
&T_{G\xi} = I_{ch\xi}\ddot{\alpha} \\
&T_{G\eta} = I_{ch\eta}\ddot{\beta} \\
&T_{G\zeta} = I_{ch\zeta}\ddot{\gamma} \\
&T_i - F_{ri}\ R_0 = J_0\dot{\Omega}_i \qquad i=1\text{-}4
\end{aligned} \tag{19}$$

where, $\sum_{i=1}^{4} F_{\xi i}$ is the resultant in ξ direction of the actuation and resistant forces applied to the platform from the four wheels; $F_{\xi g}$ is the component in ξ direction of the gravity force; m_T is the vehicle total mass including motor wheels, suspensions and chassis; a_ξ is the acceleration of the chassis center of gravity along the ξ axis. The expressions of the forces are introduced in the next sections.

The $\sum_{i=1}^{4} F_{\eta i}$ is the resultant in η direction of the resistant forces applied to the platform from the four wheels and a_η is the acceleration of the chassis center of gravity along the η axis.

The $T_{G\xi}$ is the resultant torque on the chassis around the ξ axis due to the forces acting on the wheels and due to the suspensions; $I_{ch\xi}$ is the chassis inertia about the ξ axis.

The $T_{g\eta}$ is the resultant torque on the chassis around the η axis due to the forces acting on the wheels and due to the suspensions; $I_{ch\eta}$ is the chassis inertia about the η axis.

The $T_{G\zeta}$ is the resultant torque on the chassis around the ζ axis due to the forces acting on the wheels; $I_{ch\zeta}$ is the chassis inertia about the ζ axis.

$$T_{G\zeta} = \sum_{i=1}^{4} (-F_{\xi i}\ \eta_i + F_{\eta i}\ \xi_i) \tag{20}$$

This yawing torque guarantees to the vehicle a right behaviour in curve because it is responsible of the vehicle non stationary behaviour in curved paths along which the vehicle angular accelerations happen (Shino and Nagai, 2003).

The T_i are the wheel motors driving torques, J is the wheel inertia about the wheel axis; F_{ri} is the force tangential to the wheel due to the tyre ground contact, Ω_i are the angular velocities of the wheels.

Wheel model: The PICAV motion actuation is generated by the electric motors on the wheels. Forces at the tyre interface are not given in body axes, rather as F_{wi} components having the tyre heading and a transversal reaction (Fig. 5).

Through each tyre, traction forces $[F_{\xi i}\ F_{\eta i}]^T$, tangential F_{wni} and transversal F_{wni} reactions are applied; if δ_i are the local steering angles, these forces can be decomposed in the body frame by means of:

$$\begin{bmatrix} F_{\xi i} \\ F_{\eta i} \end{bmatrix} = \begin{bmatrix} \cos\delta_i & -\sin\delta_i \\ \sin\delta_i & \cos\delta_i \end{bmatrix} \begin{bmatrix} F_{wri} \\ F_{wni} \end{bmatrix} \tag{21}$$

Following the literature (Pacejka and Besselink, 1997) the tyre ground behaviour $[F_{\xi i}\ F_{\eta i}]^T$ at each wheel i depends on the rate of the vehicle weight loading the wheel normal to the ground $F_{\zeta i}$, the slip s_i, the adherence δ_i, the cornering stiffness C_i, the velocities of the point P_i as given in Eq. 17:

$$\begin{aligned}
&F_{wri} = \mu(s_i) F_{\zeta i} \\
&F_{wni} = C_i\ \text{sgn}(V_{Pi\eta})\ \text{atan}\left(\frac{|V_{Pi\eta}|}{|V_{Pi\xi}|}\right) \\
&s_i = \frac{\Omega_i R_0 - V_{Pi\xi}}{\Omega_i R_0}\ \text{sgn}(V_{Pi\xi}) \\
&F_{\zeta i} \simeq g\frac{m_T}{4}\cos\beta_0
\end{aligned} \tag{22}$$

where an equal distribution of the load on the four wheels has been admitted. The law $\mu(s_i)$ is approximated by a non linear saturation law, symmetric for traction and breaking regions, where the saturation value is s_{sat}. In fact the F_{wri} is due to the transversal elasticity of the tyre that first increases linearly with the slip, then slowly and slowly up to keep about constant in presence of very high slip.

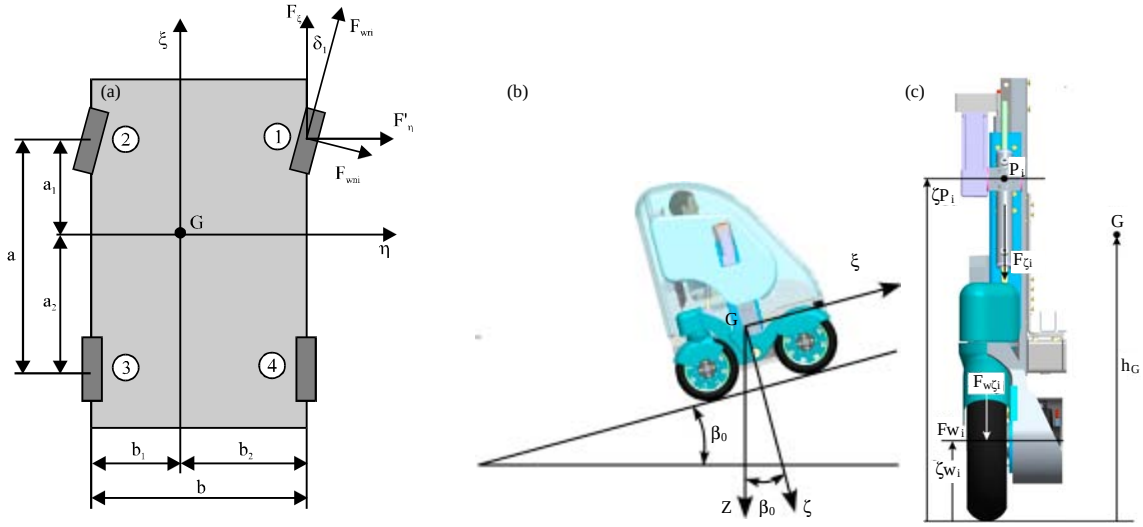

Fig. 5(a-c): Geometric parameters for the (a) Kinematic analysis and detail of the suspension, (b) Tyre heading and (c) Transversal reaction

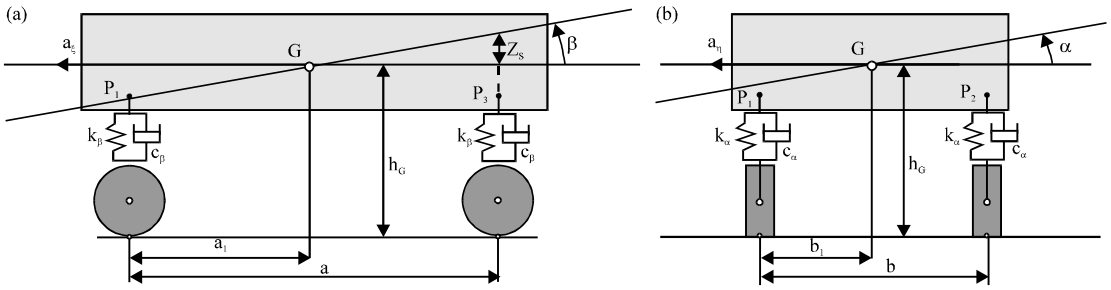

Fig. 6(a-b): Pitch and roll vehicle models. (a) Roll and (b) Pitch motions

Suspensions model: The accelerations and decelerations in ξ and η directions cause the so called load transfers that generate the roll and pitch motions.

In view of defining possible control strategies, the almost-rigid suspension model is considered. This approximation allows a distribution of the reactions with negligible dynamic cross-coupling at low velocities so, within the low speed bounds of the vehicle, each carrying suspension can be separately described.

Referring to the roll and pitch sketches of Fig. 6, the dynamic models of the roll and pitch motions can be described as:

$$\begin{aligned} &m_s a_\eta h_G = I_{ch\xi}\ddot{\alpha} + c_\alpha\dot{\alpha} + k_\alpha\alpha \\ &\text{being:} \\ &T_{G\eta} = m_s a_\eta h_G - c_\alpha\dot{\alpha} - k_\alpha\alpha \\ &m_s a_\xi h_G = I_{ch\eta}\ddot{\beta} + c_\beta\dot{\beta} + k_\beta\beta \\ &\text{being:} \\ &T_{G\xi} = m_s a_\xi h_G - c_\beta\dot{\beta} - k_\beta\beta \end{aligned} \quad (23)$$

where, m_s is the platform hanging mass without wheels and suspensions masses; h_G is the height of the platform centroid G; c_α, c_β are the suspensions damping coefficients to the roll and pitch motions and k_α, k_β are the suspensions elastic coefficients to the roll and pitch motions. $T_{G\eta}$, $T_{G\xi}$ are the torques acting on the suspended platform generated by a_η and a_ξ.

The load transfers are greater for higher center of mass and smaller a, b. Further they are influenced by the wheel ground adherence: In fact a greater adherence causes bigger acceleration and deceleration generating greater load transfer.

The steering actions can be conventionally assured by deflecting the front axle wheels; alternatively, steering can be obtained by exploiting the drifting effects induced by differential torques ratios between the wheels of the same axle.

Electric motor model: The in-wheel electric motors are modelled by:

$$V = Li + Ri + K_t\Omega$$
$$T = K_t i - K_m^2\Omega - J_m\dot{\Omega} \quad (24)$$

where, the values of the winding resistance R and inductance L, rotor inertia J_m, motor constants K_t and K_m are characteristics of the used motors, given by the supplier catalogue; T is the motor torque, V is the armature voltage and i is the current.

FUZZY-LOGIC CONTROLLER

For the present application, the control system should assure the specified travel velocity by assigning to each tyre the torque and speed consistent with the desired acceleration (along straight or curved paths). Due to the redundancy of the four powered wheels, the total actuation torque shall split in such a way that torque balance and cinematic steering is pursued with the required slip ratio between the soil and each tyre (Michelini *et al*., 2001b). The backward kinematics of car's motion, therefore, is important giving the basic reference target of the motor wheels angular velocities corresponding to the control input in terms of the path variables: the current vehicle body velocity and steering angle.

PI hybrid controller: The usual PID controllers, despite their effectiveness for simple linear systems, are generally not suitable for higher order, non-linear systems, especially when the operating conditions are quickly changing, as it is the case in the present application (Rattighieri *et al*., 2001). Thus, several modifications have been considered in the past to include a priori knowledge on the system or on the environment or some self-compensation capability to get rid of the off-setting disturbances. In particular, the fuzzy-logic PID controllers show good abilities to cope with complex non-linear MIMO systems and reference is done to this kind of adaptive controllers for its simple, easy made implementation.

In fact, fuzzy control is one of the most successful application areas of the fuzzy theory and it is effective to deal with control problems which are difficult to solve by developing precise mathematical models (Wang *et al*., 2011). A fuzzy controller consists of a set of fuzzy rules processed with a system of logic inference; the fuzzy rule base consists of a collection of rules which represents all possible situations and their corresponding control actions: the logic inference converts the linguistic labels of the rule base into a final crisp control action (Yu and Yao, 2011).

As first control scheme, a purely kinematic controller, based on a conventional PI structure, is considered. The adaptivity of the vehicle to the varying operating conditions is managed through a fuzzy block, with the main goal to bring the complex non-linear system to work near stable conditions (Fig. 7). The fuzzy controlled variables (wheels angular speeds) are compared with the reference values coming from the backward kinematic block and are used to tune the control gains in order to guarantee the required path, ensuring, at least, the vehicle theoretical kinematic steering. The control system main goal is to keep small the wheels angular velocity errors. The vehicle control system computes the four motor wheels torques applying a PI control strategy with the proportional gain K_p very larger than the integral gain K_i in order to ensure a quick behaviour avoiding noisy oscillations around the equilibrium (McKerrow, 1991); furthermore, the gains are adapted to the actual working conditions by computing, through a fuzzy block, the local adjusting factors ΔK_p and ΔK_i. In order to get significant results, yet in simulated virtual environment, the detailed vehicle model described in Vehicle model section was adopted and the electric motors contribution to the vehicle dynamic behaviour was considered.

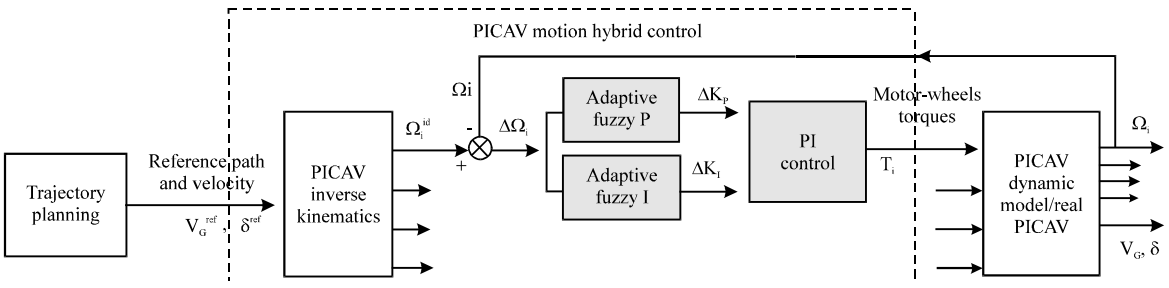

Fig. 7: Scheme of the hybrid PI/fuzzy controller

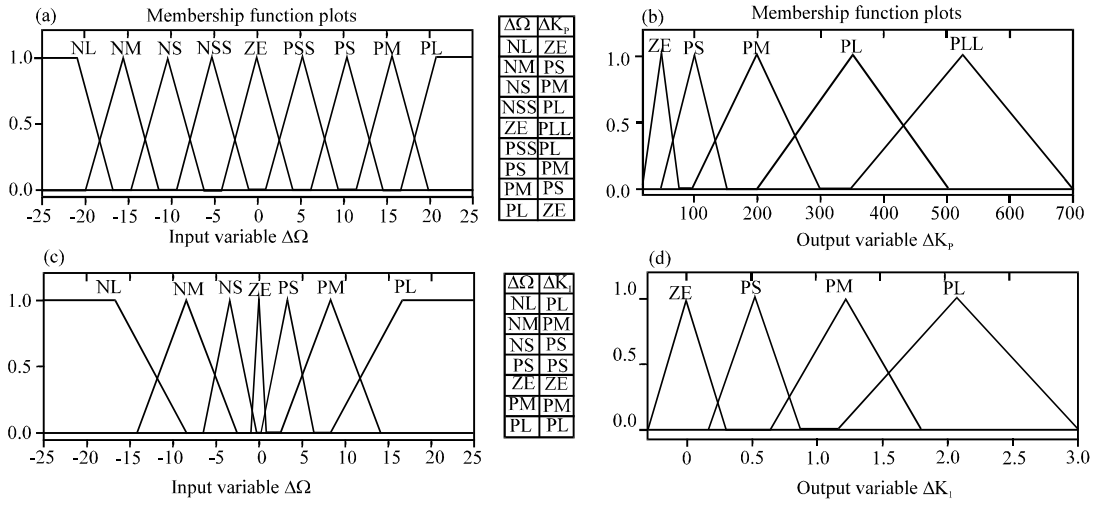

Fig. 8(a-d): Adaptive fuzzy control rules and memberships for (a, c) Input variables ($\Delta\Omega$) and (b, d) Output variables (Δk_p)

Different Membership Functions (MF) encoding human expertise about car driving have been tested and assessed with the help of the purposely developed vehicle model described in the previous section and implemented in Simulink; this kind of control demonstrated to not be significantly sensible to the MF shapes. The rules and memberships adopted are shown in Fig. 8. For example, when the actual velocities are near the reference values, the traditional PI control is less efficient and quick so the gains adjusting components are made higher to enhance the system sensibility to small errors; on the contrary, large velocity errors lead to small corresponding gains adjustments, being sufficiently high the traditional PI contributions, at least when output motor torques are far from saturation. The Center of Gravity method, Max Min rules, With Overlaps CGMMWO has been applied for the defuzzyfication of the gains increments.

The control proposed has been extensively tested in simulation under different working conditions. The authors are aware that never a simulation campaign could be complete but great attention has been dedicated to the trajectories and ground conditions significance. In the following the results of some example tests are presented. Figure 9 presents the results of test 6 where: the desired path is straightforward ($\delta = 0$), the vehicle is required to accelerate from the initial velocity of 2.1 m sec^{-1} till the velocity of 6 m sec^{-1}, the wheels-road adherence is high: $\mu = 1$ (dry road), the vehicle load is unbalanced. The velocity response is good and the settling time of 2 sec is satisfactory, Fig. 9a, the wheels velocity errors are limited and nullify in about 2 sec, (Fig. 9b). Figure 9c and d show the adaptation of the proportional and integral gains. The acceleration causes a pitch motion that nullifies as the wanted steady state conditions are achieved, as shown in Fig. 9e while the unbalanced distribution of the load on the wheels causes a light roll motion that presents the trend in Fig. 9f.

Another test here presented, test 8, refers to these conditions: The vehicle, balance, is required to accelerate from $v_0 = 7$ m sec^{-1} to $v_{id} = 8.4$ m sec^{-1} all along a curved path with steering angle increasing sinusoidally from zero degree till the maximum value of 3° that is then kept constant; the vehicle moves on dry ($\mu = 1$) regular ground. Figure 10a, reports the vehicle velocity response, the vehicle pitch and roll motions are presented in Fig. 10b, the roll motion in this case of balanced vehicle, is due to the side acceleration of the vehicle determined by the curved path; the adaptation laws of the proportional and integral gains are respectively shown in Fig. 10c and d. The trend of the torques at the wheel motor 1 is shown in Fig. 10e, similar trends apply to the other wheels; the distribution of the vertical loads variations on the four wheels. Figure 10f, shows that the external wheels 1 and 3 are more loaded than the internal ones due to the centrifugal forces.

Further tests have been performed to study the vehicle behaviour in different adherence conditions of the road. With the same path, velocity and acceleration of the reference test 6, the vehicle behaviour on different ground conditions: dry, wet, iced road surface has been studied, test 11 and some results are shown in Fig. 11. As the adherence coefficient lowers also the resistance forces on the wheels lower and the control system allows the wheel

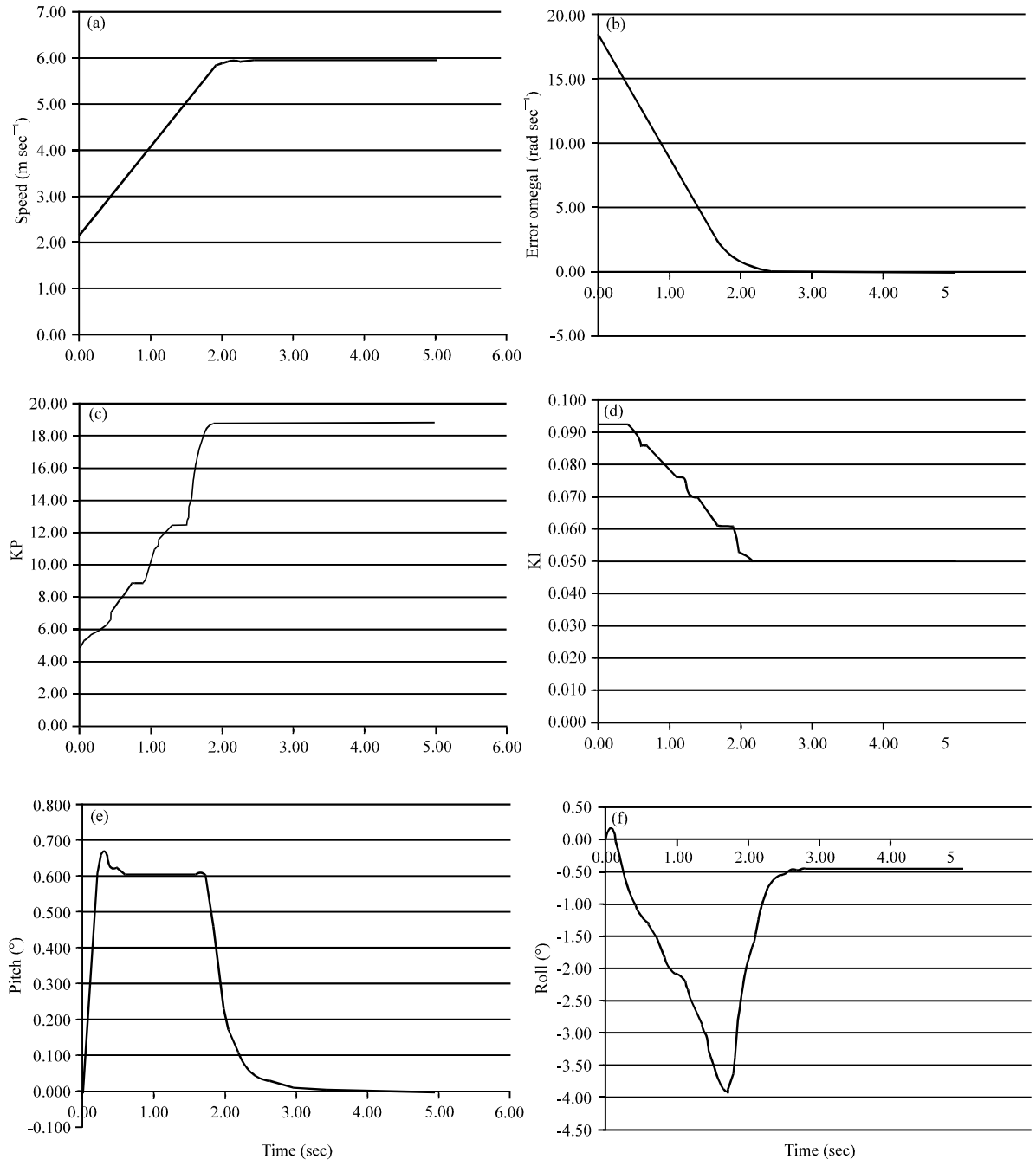

Fig. 9(a-f): PICAV behaviour on a straight path for test 6 for (a) Speed (b) Error Omega 1, (c) KP, (d) KI, (e) Pitch and (f) Roll

to reach the required velocity in less time (Fig. 11a), while in the same adherence reduction causes a reduction of the traction forces acting on the vehicle so it achieves more slowly the required speed (Fig. 11b).

Figure 12 shows the result of the test 14. The initial velocity of the vehicle is v_0 = 2.1 m sec^{-1}, v_{id} = 6 m sec^{-1}, the steering angle follows a sinusoidal law till a maximum steering angle of δ_{max} = 5°, the wheels-road adherence is low (μ = 0.2). The loss of adherence of two wheels (higher derivative of the angular velocities) can be noted from Fig. 12a. Figure 12b shows the trend of the vertical loads on the wheels.

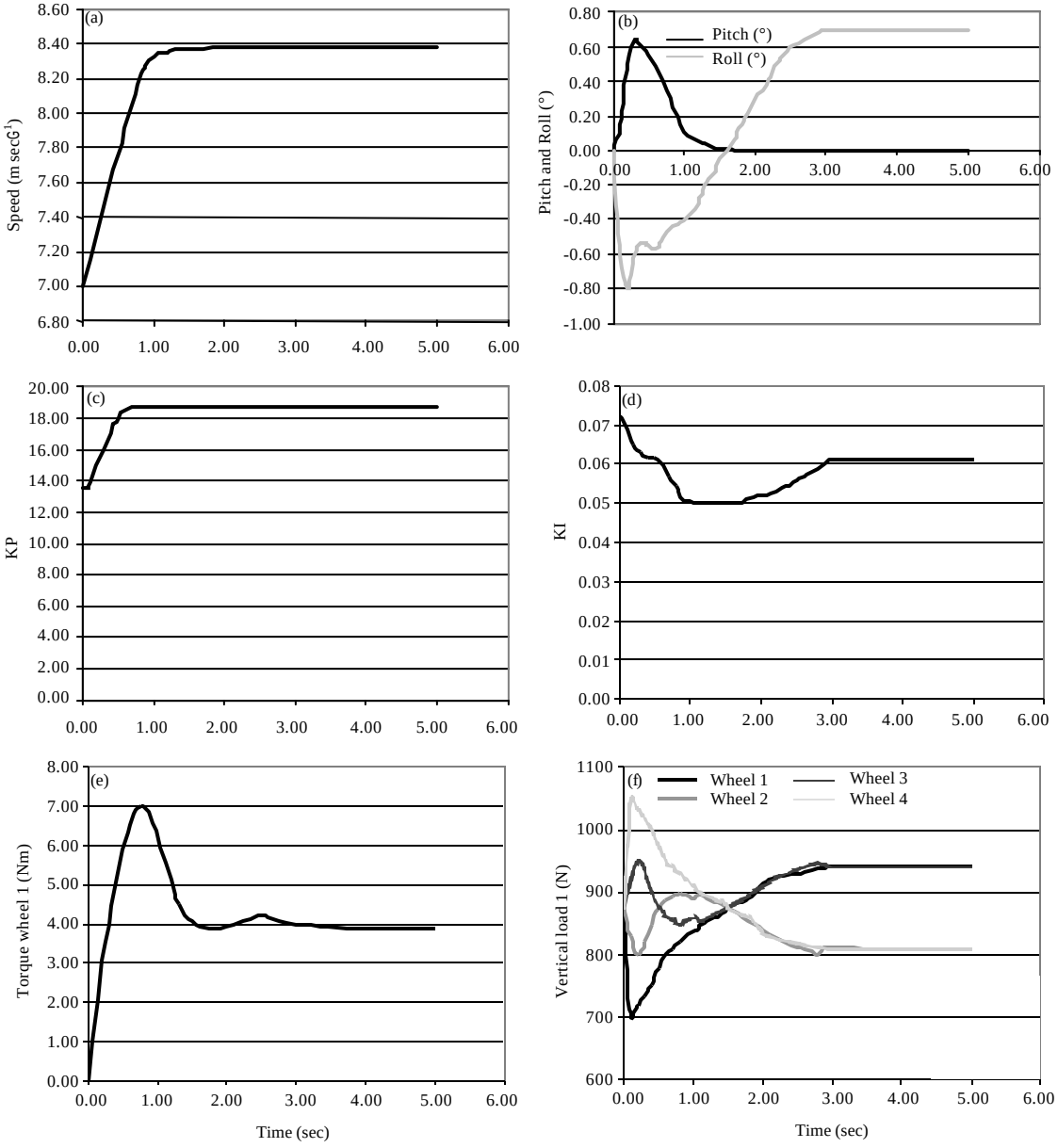

Fig. 10(a-f): PICAV behaviour along curved path for test 8 for (a) Speed (b) Pitch and Roll, (c) KP, (d) KI, (e) Torque wheel 1 and (f) Vertical load

The test campaign showed that when the vehicle speed is limited under 25 km h^{-1}, so that the hypothesis of kinematic steering is verified and the soil presents homogeneous conditions under the four wheels (as it usually happens, e.g., for cars running over well maintained roads), the control performance is satisfying.

If these hypotheses are not verified, the control may become critical or even be lost. While the first hypothesis is acceptable for PICAV, the second is not satisfying the typical operative conditions of a personal car to be used in city centers and parks.

Fully fuzzy controller: To overcome these limits, that are mainly evidenced in split road conditions, an upgrading of previous scheme is proposed, by introducing, as second fuzzy input, the slip ratio, defined as:

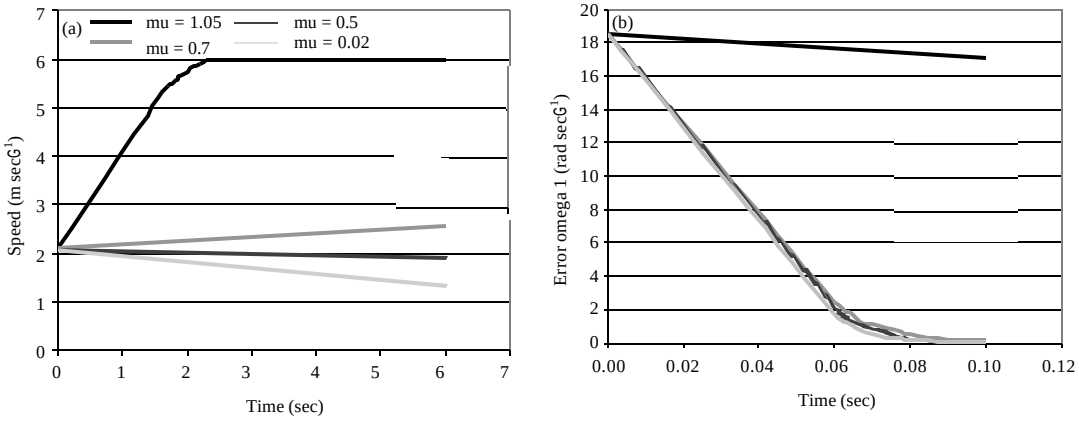

Fig. 11(a-b): PICAV behaviour on different ground conditions for test 11 for (a) Speed and (b) Error Omega 1

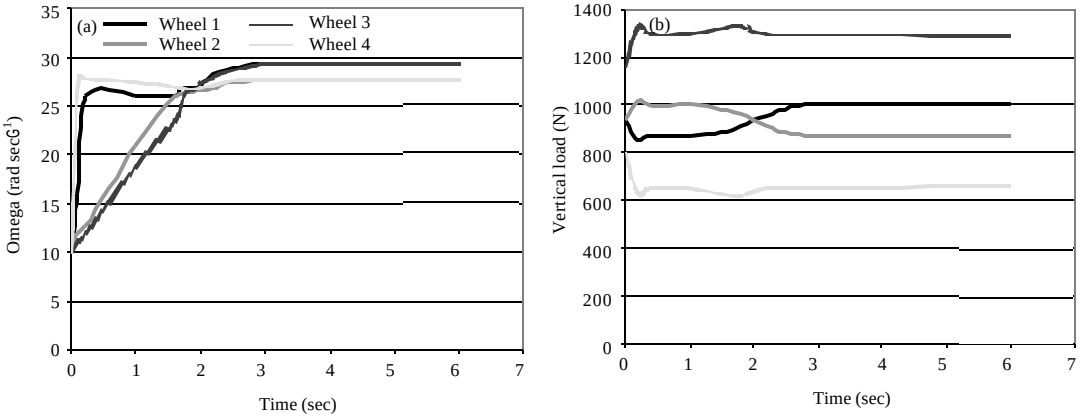

Fig. 12(a-b): Hybrid control: (a) Angular velocities and (b) Vertical loads variations on the four wheels in a typical test with vehicle steering

$$s_i = \frac{\Omega_i R_0 - V_{Pi\xi}}{\Omega_i R_0} \operatorname{sgn}\left(V_{Pi\xi}\right) \quad \Omega_i \neq 0 \tag{25}$$

according to the computational definition of (Pacejka and Besselink, 1997) and evaluated by the slip estimator block using the vehicle model introduced in Vehicle dynamic model section. In this definition the slip ratio is positive when the vehicle is accelerating and negative when it is braking. In such a way, as long as the soil contact allows the transmission of the required forces, the target kinematic conditions are pursued, but when one or more tyres tend to run out the adherence limits, the fuzzy rules extension grants the stability of cruise, despite the required vehicle's velocity and road conditions. This high stability and easy drivability performance is really appreciated in a vehicle like PICAV that is purposely designed to guarantee the accessibility to all people, older and disabled included. The fully fuzzy control sketch is shown in Fig. 13.

The fuzzyfication of $\Delta\Omega_i$ and s_i is a critical operation because the selection of the relative MFs has a great influence on the performances of the fuzzy controller (Fraichard and Garnier, 2001). The selection of the MF was made through virtual experiments using the set up Simulink parametric model, guided by a heuristic search.

As an example hereafter are compared the vehicle performances obtained using two different fuzzy sets defined on the same input variables domain and working with the same rules, as shown in Fig. 14 and 15.

All the MF are triangular shaped in the variable $\Delta\Omega$ varying in the range±20 rad sec^{-1}; both sets use 7 MFs presenting a finer discretization at small values in set 1 while for the slip ratio, varying in the range ±0.6, both sets use 5 symmetric Mfs presenting a finer discretization at

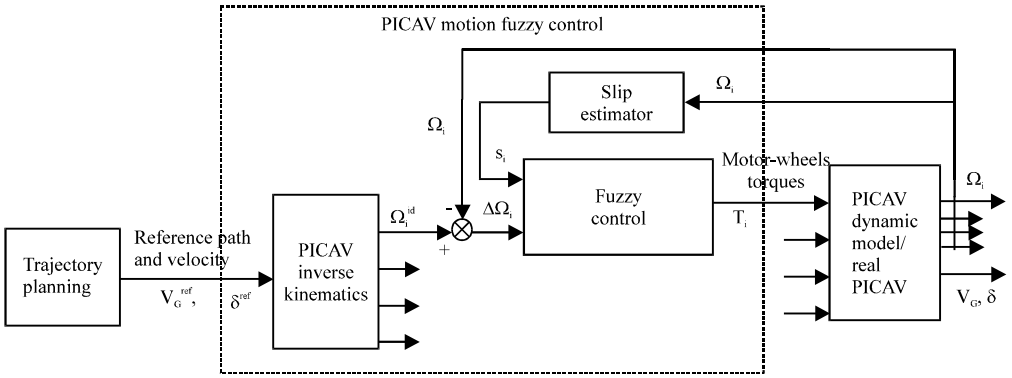

Fig. 13: Fuzzy controller

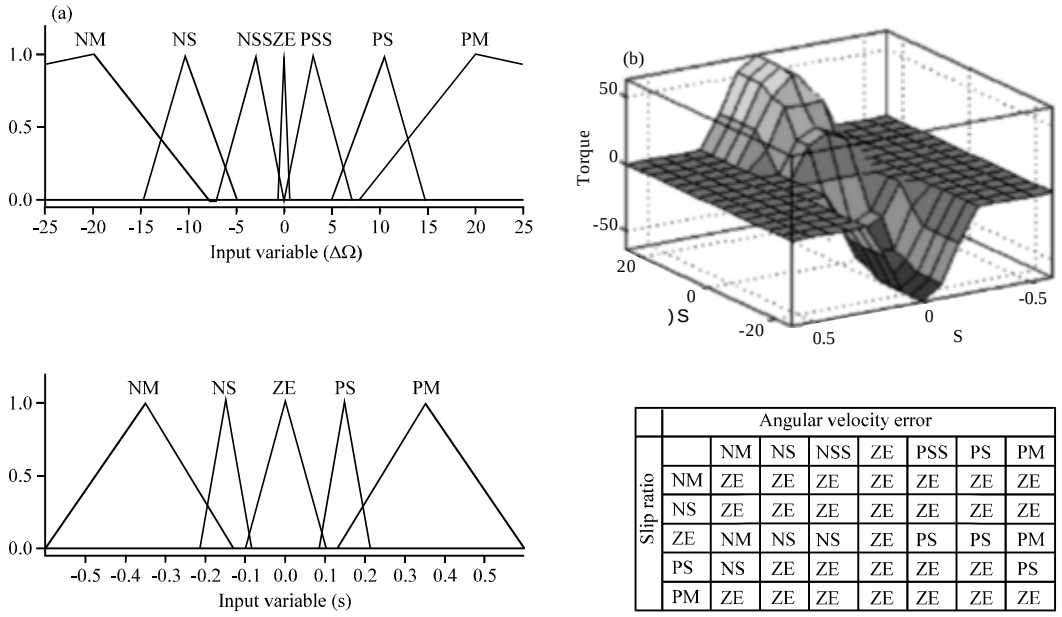

Slip ratio \ Angular velocity error	NM	NS	NSS	ZE	PSS	PS	PM
NM	ZE	ZE	ZE	ZE	ZE	ZE	ZE
NS	ZE	ZE	ZE	ZE	ZE	ZE	ZE
ZE	NM	NS	NS	ZE	PS	PS	PM
PS	NS	ZE	ZE	ZE	ZE	ZE	PS
PM	ZE	ZE	ZE	ZE	ZE	ZE	ZE

Fig. 14(a-b): Set 1 (a) Membership functions and rules and (b) Torque response surface for the fully fuzzy controller

small values in set 2. The results obtained on PICAV following a rectilinear track on icy ground ($\mu = 0.1$) with initial and final velocities respectively $V_i = 2.1$ m sec^{-1} and $V_f = 6.0$ m sec^{-1}. are shown in Fig. 16 and it can be noticed that the behaviour of the vehicle in the case of adoption of set 1 is better.

Triangular shaped membership functions are adopted both for the input variables: The wheel angular velocities, with the same granularity of the previous control and the slip ratio, as indicated in Fig. 15a, as well as for the output variable, the driving torques. In Fig. 15b, the usual pattern of the 'fuzzy associative memory' for this control scheme is shown. It is observed that, if the local sliding is low (ZE), the driving torques have the same level of the wheel angular velocity; so pretty high torques (PM) can be applied to cope with high velocity errors (PM). Instead, in case of limited slip conditions (PM), the torques need, anyway, be low (ZE). The shape of the membership functions shall be tuned according to the expected performance of the vehicle: The slip ratio, for instance, should be made with sharp edges triangles (i.e., short bases and thus, low torques) to enhance safety conditions, while large base triangles should be chosen for high speed performances. Figures 14b and 15b show the response surfaces of the control system, that is the entire span of the output set (motor's torque) based on the entire span of the input sets (slip and error on angular velocity).

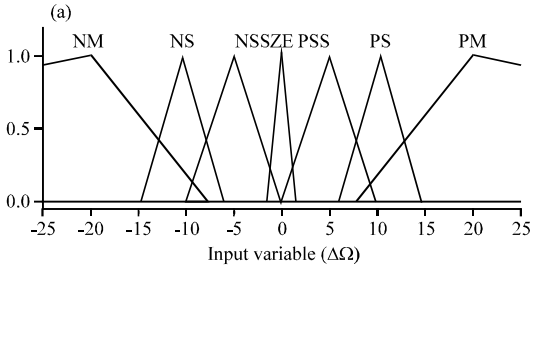

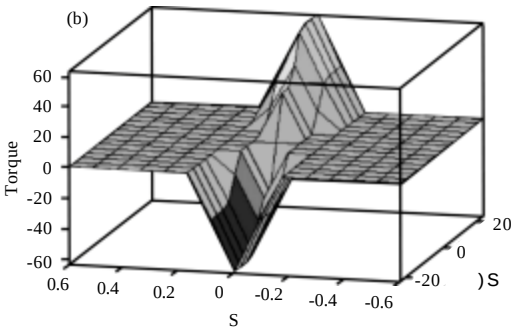

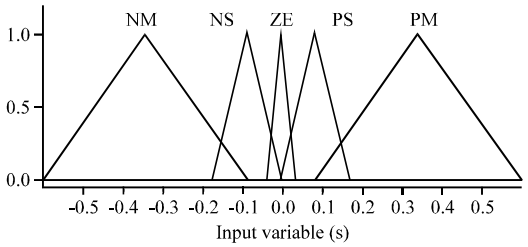

Slip ratio	Angular velocity error						
	NM	NS	NSS	ZE	PSS	PS	PM
NM	ZE	ZE	ZE	ZE	ZE	ZE	ZE
NS	ZE	ZE	ZE	ZE	ZE	ZE	ZE
ZE	NM	NS	NS	ZE	PS	PS	PM
PS	NS	ZE	ZE	ZE	ZE	ZE	PS
PM	ZE	ZE	ZE	ZE	ZE	ZE	ZE

Fig. 15(a-b): Set 2 (a) Membership functions and rules and (b) Torque response surface for the fully fuzzy controller

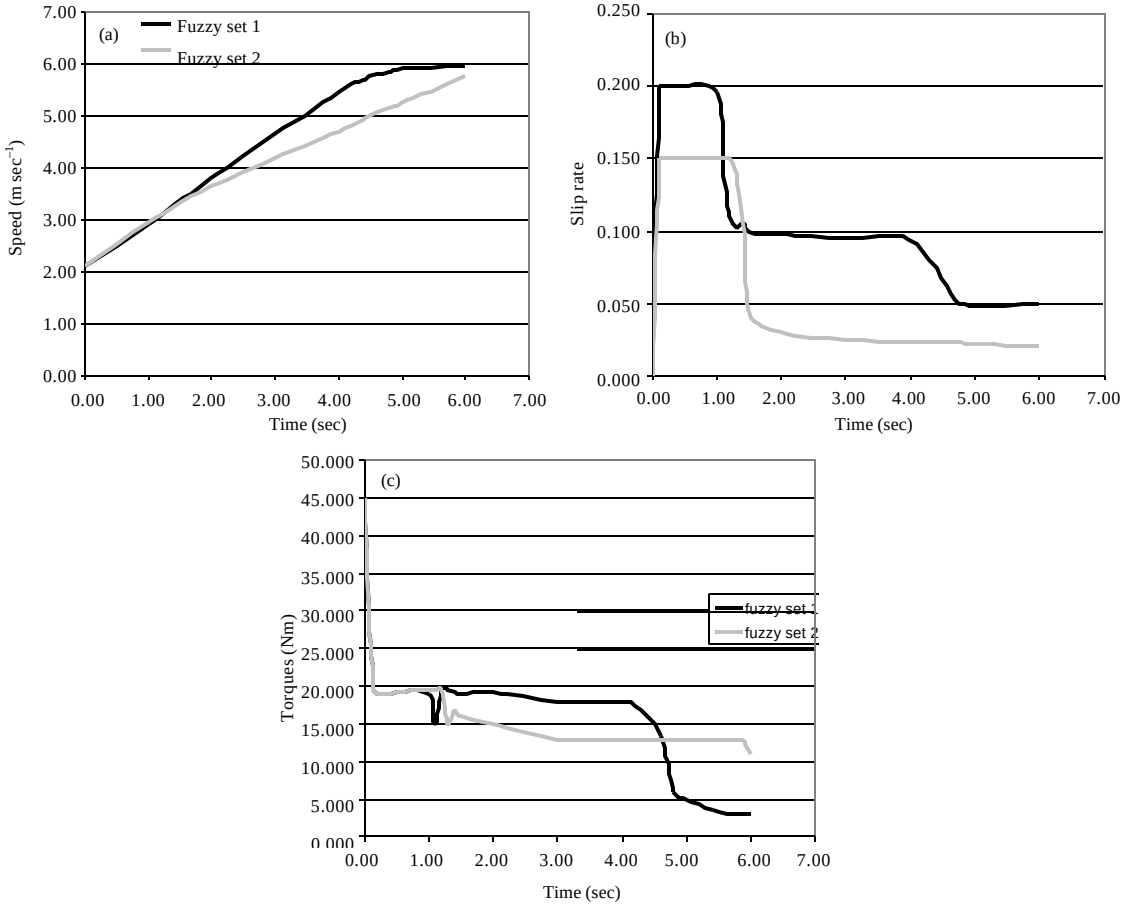

Fig. 16(a-c): Comparison between the results obtained using Fuzzy sets 1 and 2 for (a) Speed (b) Slip rate and (c) Torque

The simulation tests show that this control scheme is capable of keeping all the wheels adherent assuring the slip ratio beyond the 12-16% values, that represent the limit condition of wheel's spinning.

As an example, results achieved with the fully fuzzy control system in the same operative conditions of test 14 and reported in Fig. 10 are shown in Fig. 17.

The simulation test campaign related to the fully fuzzy controller shows to be an improvement with respect to the previous formulation and provides the advantage of requiring less sophisticated tuning and dynamic based decisions. The already performed test of vehicle's acceleration along a straight path is repeated with the new controller and from the comparison of the results, it can be seen that the slip ratio keeps about constant satisfying the limit conditions, while it varied a lot on time with the original setting; on the other hand, of course, the target velocity is reached after a longer time, due to the lower traction force that is now supplied.

The second PICAV prototype has been realized and integrated, as shown in Fig. 18a. Experimental tests have been performed open loop, human driven and closed loop, driven through the fully fuzzy control system set 1 membership functions.

The same operative conditions of the test 21, slight acceleration on rectilinear track on icy ground, have been reconstructed and the velocity of the vehicle was monitored. In Fig. 18b the monitored velocity of the vehicle is compared to the corresponding results obtained through the simulation. The comparison of the vehicle simulated and monitored speed relative to test 24, fuzzy MF1 control, same curved track of test 8 on dry ground are shown in Fig. 18c.

The obtained results seem to confirm the satisfactory behaviour achieved by the fuzzy control system through the virtual tests.

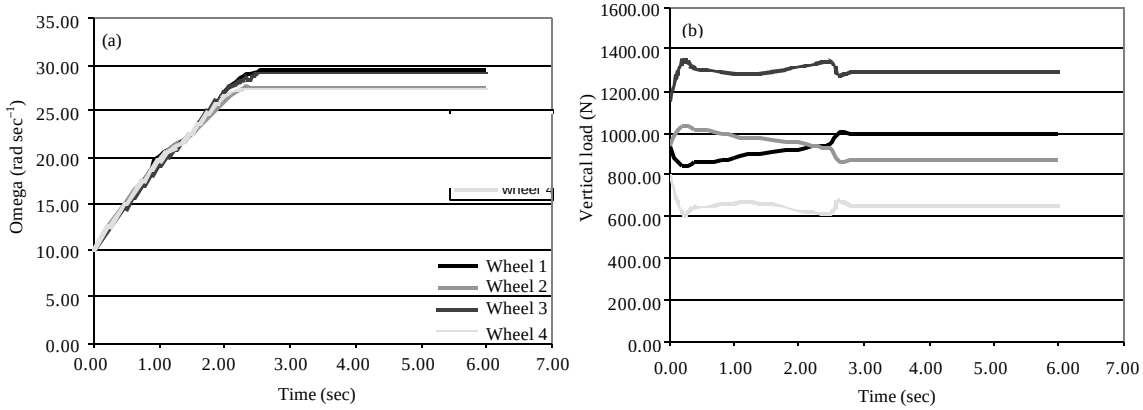

Fig. 17(a-b): Fully fuzzy control: (a) Angular velocities and (b) Vertical loads on the four wheels in a typical test with vehicle steering. No loss of adherence of the wheels

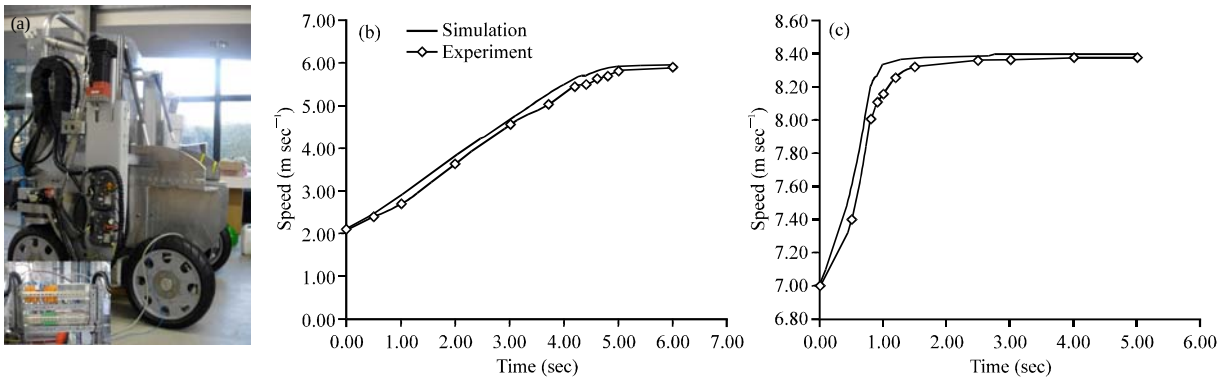

Fig. 18(a-c): (a) Experimental tests: testing arrangement, (b) Comparison between the simulated and measured velocity of the vehicle in rectilinear path with test 21 conditions and (c) Comparison between the simulated and measured velocity of the vehicle in curved path with test 24 conditions

CONCLUSIONS

The study presents results about explorations performed along the design of the control strategy of the PICAV vehicle, taking into account urban scenario strategies (Cepolina and Farina, 2012b). It exploits two non linear controller based on fuzzy logics. The set-up profits by the inclusion of a fuzzy-logic supervisor, with two aims: (1) To grant stability in front of process uncertainties (road slipperiness and unevenness, etc) and (2) To supply a friendly restitution of the steering commands, so that the user keeps self-confidence of the tyres' controlled slip mechanism.

For robotized vehicles, like PICAV, the control is not necessarily always an open-loop system, with a human driver closing the loop and supervising steering and braking actions. The proposed approach in control design is oriented to semi-autonomous and autonomous driving. In effect the knowledge of the vehicle status conditions, achieved through the sensors, is used to assist the driver in order that steering and/or braking commands stay inside the friction cone, improving the vehicle safe motion. On the other side, a completely autonomous vehicle needs a more sophisticated mechatronic design that offers intrinsic stability and robustness to internal and external disturbances based on the non linear control layer that has been analysed in this study.

ACKNOWLEDGMENTS

The study is developed within the PICAV project funded under the Seventh Framework Program (Collaborative Project SCPS-GA-2009-233776). We kindly acknowledge the funding and assistance of the European Commission.

REFERENCES

Cepolina, E.M. and N.A. Tyler, 2001. Microscopic simulation of pedestrians in accessibility evaluation. Transp. Plann. Technol., 27: 149-180.

Cepolina, E.M. and A. Farina, 2012a. A new shared vehicle system for urban areas. Transp. Res. Part C, 21: 230-243.

Cepolina, E.M. and A. Farina, 2012b. Urban Car Sharing: An Overview of Relocation Strategies. In: Urban Transport XVIII, Chapter: Urban Car Sharing: An Overview of Relocation Strategies, WIT Press (Eds.). JWS Longhurst, UK., ISBN: 9781845645809, pp: 419-432.

Fraichard, T. and P. Garnier, 2001. Fuzzy control to drive car-like vahicles. Robotics Autonomous Syst., 34: 1-22.

Grzegozek, W., 2010. Personal commuting vehicle concept. J. KONES Powertrain Transp., 17: 113-118.

Kato, Y., M. Hosokawa and M. Morita, 2006. Future personal mobility i-unit. J. Soc. Automot. Eng. Japan Intell. Transp. Syst., 60: 97-102.

Lark, W., 2005. City-Car: Optimizing vehicle and urban efficiencies through a shared adaptive platform. M.Sc. Thesis, Massachusetts Institute of Technology, Department of Architecture. Program in Media Arts and Sciences.

McKerrow, P.J., 1991. Introduction to Robotics: (Electronic Systems Engineering Series). Addison-Wesley Pubication, New York, ISBN-13: 978-0201182408, Pages: 800.

Michelini, R.C., R.M. Molfino, R. Ghigliazza and M. Callegari, 2001a. Dynamic characterisation of a city-car with innovative actuation and manoeuvrability for restricted urban traffic. Proceedings of the 2nd International Colloquium on Vehicle Tyre Road Interaction, Friction Potential and Safety: Prediction of Handling Behavior, February 23, 2001, Florence, pp: 1-5.

Michelini, R.C., R.M. Molfino, R.E. Ghigliazza and M. Callegari, 2001b. The tyre-soil effects on the manoeuvrability of a city-car. Proceedings of the IEEE/ASME International Conference on Advanced Intelligent Mechatronics, Volume, 1, July 8-12, 2001, Como, pp: 428-433.

Mitchell, W.J., C.E. Borroni-Bird and L.D. Burns, 2010. Reinventing the Automobile: Personal Urban Mobility for the 21st Century. MIT Press, USA., ISBN-13: 978-0262013826, Pages: 240.

Pacejka, H.B. and I.J.M. Besselink, 1997. Magic formula tyre model with transient properties. J. Vehicle Syst. Dynamics: Int. J. Vehicle Mech. Mobility, 27: 234-246.

Rattighieri, G., F. Gucciardi and M. Callegari, 2001. Dynamic modelling of an electric city-car and proposal of an integrated drive-by-wire controller. Proceedings of the 7th International Conference High-Tech Cars and Engines, May 31st-June 1st, 2001, Democenter, Modena.

Rodic, A.D. and M.K. Vukobratovic, 1996. Model based control of road vehicles as robotized dynamic systems. Proceedings of the 2nd ECPD International Conference Advanced Robotics, Intelligent Automation and Active Systems, September 26-28, 1996, Vienna, pp: 612-614.

Saiz-Rubio, V., F. Rovira-Mas, I. Chatterjee and J.M.M. Hidalgo, 2013. Robust estimation of Ackerman angles for front-axle steered vehicles. Artif. Intell. Res., 2: 18-27.

Sawatzky, B., I. Denison, S. Langrish, S. Richardson, K. Hiller and B. Slobogean, 2007. The Segway personal transporter as an alternative mobility device for people with disabilities: A pilot study. Arch. Phys. Med. Rehabil., 88: 1423-1428.

Shino, M. and M. Nagai, 2003. Independent wheel torque control of small-scale electric vehicle for handling and stability improvement. JSAE Rev., 24: 449-456.

Wang, B., R. Wang, H. Sun and Q. Cai, 2011. Simulation research on vehicle stability control for 4WD electric vehicle. Proceedings of the 3rd International Conference on Measuring Technology and Mechatronics Automation, Volume 3, January 6-7 2011, Shangshai, pp: 274-277.

Yu, C.Z. and Z.G. Yao, 2011. Fuzzy control strategy and simulation for dual electric tracked vehicle motion control. Applied Mech. Mater., 130-134: 309-312.